International Journal of Mechanical, Industrial and Aerospace Sciences
ISSN: 2517-9950
Vol:14, No:7, 2020

Heat and Mass Transfer Modelling of Industrial Sludge Drying at Different Pressures and Temperatures

L. Al Ahmad, C. Latrille, D. Hainos, D. Blanc, M. Clausse

***Abstract*—**A two-dimensional finite volume axisymmetric model is developed to predict the simultaneous heat and mass transfers during the drying of industrial sludge. The simulations were run using COMSOL-Multiphysics 3.5a. The input parameters of the numerical model were acquired from a preliminary experimental work. Results permit to establish correlations describing the evolution of the various parameters as a function of the drying temperature and the sludge water content. The selection and coupling of the equation are validated based on the drying kinetics acquired experimentally at a temperature range of 45-65 °C and absolute pressure range of 200-1000 mbar. The model, incorporating the heat and mass transfer mechanisms at different operating conditions, shows simulated values of temperature and water content. Simulated results are found concordant with the experimental values, only at the first and last drying stages where sludge shrinkage is insignificant. Simulated and experimental results show that sludge drying is favored at high temperatures and low pressure. As experimentally observed, the drying time is reduced by 68% for drying at 65 °C compared to 45 °C under 1 atm. At 65 °C, a 200-mbar absolute pressure vacuum leads to an additional reduction in drying time estimated by 61%. However, the drying rate is underestimated in the intermediate stage. This rate underestimation could be improved in the model by considering the shrinkage phenomena that occurs during sludge drying.

***Keywords*—**Industrial sludge drying, heat transfer, mass transfer, mathematical modelling

I. Introduction

THE treatment of wastewater, resulting from nuclear energy production, is based on the co-precipitation of radioelements with mineral salts [1]. This process leads to a wet solid phase or sludge production, which must then be dried before storage in order to be compact and chemically stable. The industrial process consists of sludge drying inside a final receiving container in a temperature-controlled environment at 65 °C. In this context, it is essential to provide elements to define the drying time beyond which the final dryness target will be reached. To predict the behavior of sludge during water removal, a numerical model is developed using COMSOL-Multiphysics 3.5a. This model is established to simulate the drying process by considering the drying parameters identified on 30 g sludge drying tests carried out at different temperatures and vacuum pressures. These mechanisms are identified as heat and mass transfers that occur simultaneously in the porous medium of the sludge [2]-[4].

Mass transfer takes place mainly by diffusion/capillarity and depends on the temperature and the water contents gradients. The transport of water inside the porous media takes place by liquid diffusion/capillary flow (liquid water) and molecular/Knudsen diffusion (water vapor). In order to simplify the modeling of water transport, the non-isothermal water flow in the unsaturated pores of the sludge is described by Richard's equation, expressed with an apparent moisture diffusion coefficient. The apparent diffusion coefficient incorporates all the water transfer mechanisms that depend on the water content and the temperature [5]. Evaporation occurs on the liquid-gas interface and is mathematically represented by a sink term in the mass transfer equation. Evaporation stops when the local surface vapor pressure becomes less than or equal to the partial vapor pressure in the surrounding air (where the partial vapor pressure in the air is symbolized by P_G). Heat is supplied through the walls (side, top and bottom) from the hot outside environment maintained at a constant temperature (65 °C). Heat transfer takes place from the external hot zone to the inside of the sludge by conduction. The supplied heat causes the evaporation of the water. In general, thermal conduction in a porous medium is in accordance with the Fourier law [6], where latent heat is equal to the heat consumed by evaporation and is mathematically represented by a sink term in the heat transfer equation.

For modeling, the sludge is represented by a mesh of finite volumes, of which each finite volume contains three fractions: liquid, gas and solid. During sludge drying, the gas volume fraction increases with the decrease of the liquid volume fraction due to water evaporation. The solid volume fraction is considered constant for now, where shrinkage phenomenon is still not taken into account. The input data for the numerical model were acquired in a preliminary study that provides chemical/physical characteristics and thermo-physical properties of the sludge. Thus, the aim of this work is to check the coupling equations of this numerical model with simulations at different temperature and pressure conditions

F L. Al Ahmad is with Den-Service d'Etude du Comportement des Radionucléides, CEA, Université Paris-Saclay, F91191, Gif-sur-Yvette, France; and with Univ-Lyon, CNRS, INSA-Lyon, Université Claude Bernard Lyon 1, CETHIL UMR5008, F-69621, Villeurbanne, France (e-mail: layth.alahmad@cea.fr).

C. Latrille and D. Hainos are with Den-Service d'Etude du Comportement des Radionucléides, CEA, Université Paris-Saclay, F91191, Gif-sur-Yvette, France.

D. Blanc is with Univ-Lyon, INSA-Lyon, DEEP EA7429, F-69621, Villeurbanne, France (e-mail: denise.blanc-biscarat@insa-lyon.fr).

M. Clausse is with Univ-Lyon, CNRS, INSA-Lyon, Université Claude Bernard Lyon 1, CETHIL UMR5008, F-69621, Villeurbanne, France.

and to criticize the mismatches between simulations of the considered sludge drying process and experimental results.

II. Materials and Methods

A. Material and Experimental Methods

In the frame of the numerical model development and validation, an experimental apparatus is set up to measure the loss of sludge mass over time during drying. Drying is carried out at controlled/constant temperature, pressure and relative humidity conditions until equilibrium is reached. Two sets of the acquired kinetic data led to the determination of some input parameters of the model (apparent water diffusion coefficient, drying rate, etc.). The first set includes the kinetics at relative humidity (RH) = 46%, atmospheric pressure and temperatures T 45, 55, 65 °C. While the second set contains the kinetics at RH = 46%, 65 °C and absolute pressures 200, 350, 1000. On the other hand, kinetic data at RH = 46%, atmospheric pressure and 35 °C are used, in addition to the two sets, to validate the numerical model by comparing the experimental results with the numerical results.

The sludge is synthetized by salt co-precipitation. It is initially formed of a solid phase ($Ti(OH)_4$, $Fe,Ni(CN)_6K_4$, $BaSO_4$ and CoS) and a liquid phase composed of water and soluble salts, $NaNO_3$ and Na_2SO_4. The initial specific water content is 21% (kg water. kg^{-1} dry basis). The main batch of sludge is kept in a closed container to prevent loss of water during the study period.

Drying tests of 30 g sludge samples were carried out at different operating conditions: RH = 46%, 35 < T < 65 °C and 200 < P_{abs} < 1000 mbar. The sludge sample is confined in a desiccator, partially filled with a saline solution ($MgCl_2$), which imposes a constant RH. This desiccator is placed in an oven at a constant temperature (T) and a fixed absolute pressure (P_{abs}). The oven is connected to a pump and equipped with temperature and pressure control systems that maintain the operating conditions constant during the drying test. The mass measured by the balance is recorded continuously. In addition, the temperature, pressure and the RH are recorded by sensors placed inside the desiccator.

B. Mathematical Model

The model is based on the differential mass and energy balances of the sludge, which is considered in this model as a non-shrinkable medium. Thus, sludge is considered as a porous solid whose water content and temperature vary over time.

1) Model Assumptions

The main assumptions are:

- The sludge's geometry is 2D axisymmetric cylinder.
- The initial water and temperature distributions are considered uniform.
- The initial sludge porosity is uniform. The initial gas volume fraction is null all over the sludge.
- Mass and heat fluxes are considered as 2D axisymmetric.
- Heat transfer is only by conduction and heat dissipation is by evaporation.
- The RH of the surrounding air is considered constant over time.
- The sludge pores are considered sufficiently large to be connected to the surrounding air, so that the water vapor pressure in the gaseous fraction of each finite volume is equal to the water vapor pressure PG in the surrounding air.
- The physical properties of the sludge are considered dependent on the local water content.
- A statistical analysis is performed to determine the agreement between the model and the experimental values from the coefficient of determination (R2) and the root mean square error (RMSE).

2) Governing Equations

Based on these assumptions, the system of partial differential equations (PDE) is composed of a mass balance in the water phase and an energy balance on the sludge without any geometric deformation. The two PDEs are coupled by the term of the evaporation rate in the sludge. Fig. 1 shows the heat and mass transfers in the sludge and across its boundaries (1, 2, 3 and 4).

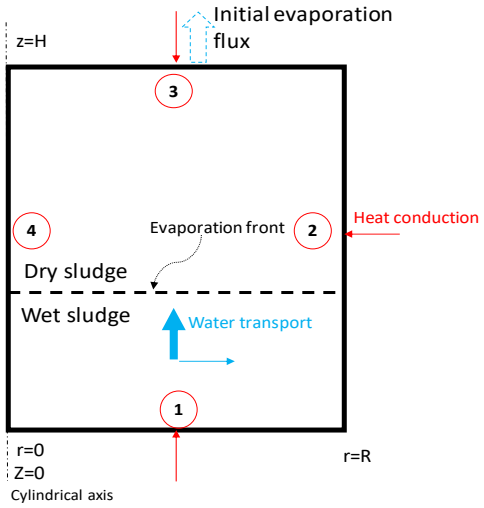

Fig. 1 Mechanisms of heat and mass transfer within the sludge during drying

The water transport is represented in (1) by Richard's equation with an apparent diffusion coefficient (m^2/s) D_{app} (X,T) dependent on water content X (-) and temperature T (°C) [5]:

$$\frac{\partial X}{\partial t} = \nabla.\left(D_{app}(X,T)\nabla X\right) - \frac{\dot{m}}{\rho_L} \quad (1)$$

where, t is time (s), $\dot{m}$ is the evaporation rate (s^{-1}) and ρ_L is the water density ($kg \cdot m^{-3}$).

Sludge is initially considered as a porous medium saturated with water. Indeed, evaporation is initiated only on the top boundary in contact with air (#3). Based on the water transport between the mesh finite volumes, new gas volume fractions

appear in the other finite volumes that initiate water evaporation gradually. Therefore, an additional equation is needed to count the gas volume fraction θ_G(-) that frames the water evaporation:

$$\Theta_L + \theta_G + \theta_S = 1 \quad (2)$$

Since the solid volume fraction θ_S (-) is supposed to be constant and the liquid volume fraction θ_L is a state variable (calculated from water content) and therefore known in each time and location, θ_G can be calculated as a complement to one.

The local evaporation rate $\dot{m}$ (s^{-1}) is supposed to be proportional to the difference between the vapor pressure in the gaseous fraction and the surface vapor pressure at the liquid-vapor interface of each finite volume [7].

$$\dot{m} = \begin{cases} K_{vap}\rho_L \frac{(a_w(X)\times P_{vap}(T)-P_G)}{P_G} \text{ if } \theta_G > 0 \text{ and } X > X_e \\ 0 \text{ if } \theta_G = 0 \text{ or } X \le X_e \text{ or } P_{vap} < P_G \end{cases} \quad (3)$$

where k_{vap} (s^{-1}) is the kinetics evaporation term, a_w (-) is the water activity, P_{vap} is the surface vapor pressure (mbar) and X_e (-) is the equilibrium water content.

The value of K_{vap} varies according to the operating conditions imposed during drying (pressure, temperature and RH). Based on the experimental kinetic data, K_{vap} values are listed in a table as function of the operating conditions. This table is inserted in the numerical model as input data.

The saturation vapor pressure P_{vap} (Pa) can be determined from the Antoine equation [8]:

$$\log_{10}(P_{vap}) = A - \frac{B}{C+T} \quad (4)$$

The heat transfer in the sludge is represented in (5) by the Fourier law with an effective thermal conductivity K_{eff} and a thermal capacity C_p that depend on the local water content. The heat dissipation is represented by the latent heat of evaporation ΔH_{vap}(J·kg^{-1}) multiplied by the evaporation rate. ρ_{app} is the apparent density of the sludge (kg·m^{-3}).

$$\rho_{app} c_p \frac{\partial T}{\partial t} = \nabla.\left(K_{eff}\nabla T\right) - \dot{m}\Delta H_{vap} \quad (5)$$

3) Initial and Boundary Conditions

Table I shows the initial and boundary conditions applied to the numerical model. The initial conditions for the two state variables (X and T) are based on the assumption of a uniform initial distribution of water content X_0 and temperature T_0 in the sludge. For the mass balance (1), the boundary conditions are expressed in axial symmetry (#4) and impose the absence of mass flow (zero flux) through the bottom and lateral boundaries (#1 and #2) whereas at the top boundary (#3), the water flux depends on the surface area that is normal to the direction of water transport. Similarly, the energy balance (5) has a constant temperature on the walls of the cylinder (boundaries #1, #2 and #3) imposed by the external environment (T_h) and an axial symmetry (#4).

TABLE I
INITIAL AND BOUNDARY CONDITIONS OF THE NUMERICAL MODEL

Boundaries #	Coordinates (r,z) or time (t)	Mass balance	Energy balance
-	$t = 0\ s$	$X = X_0$ $\theta_{G0} = 0$	$T = T_0$
1	$z = 0$	$\nabla(X) = 0;\ \nabla = [\frac{\partial}{\partial r}, \frac{\partial}{\partial z}]$	$T = T_h$
2	$r = R$	$\nabla(X) = 0;\ \nabla = [\frac{\partial}{\partial r}, \frac{\partial}{\partial z}]$	$T = T_h$
3	$z = H$	$v_{top} = -\frac{\dot{m} \times V}{A_{top}}$	$T = T_h$
4	$r = 0$	$\frac{\partial X}{\partial r} = 0$	$\frac{\partial T}{\partial r} = 0$

4) Input Data

Table II shows a summary of the sludge properties and input data for the model, determined experimentally or by other relationships retrieved from the literature.

TABLE II
INPUT DATA OF THE NUMERICAL MODEL

Parameters	Expression	Unit	Description
R	1.8	cm	Sludge radius (30 g samples)
H	2.2	cm	Sludge height (30 g samples)
A	8.07	-	Constants in Antoine equation [8]
B	1730.63	K	
C	233.43	K	
ρ_L	1000	kg·m^{-3}	Water density
T_0	25	°C	Sludge initial temperature
T_h	65	°C	Outside temperature
X_0	2.1	-	Initial water content
RH	46	%	Relative humidity
P_{abs}	[200-1000]	mbar	Absolute pressure
PG	$RH \times 133.32 \times P_{abs} \times 10^{(A-\frac{B}{C+(T-273.15)})}$	Pa	Vapor pressure in the surrounding air
P_{vap}	$133.32 \times 10^{(A-\frac{B}{C+(T-273.15)})}$	Pa	Saturation vapor pressure [8]
K_{eff}	$0.98\frac{X}{X_0} + 1.62$	W·m^{-1}·K^{-1}	Effective thermal conductivity
ρ_0	1350	kg·m^{-3}	Initial apparent sludge density
ρ_{app}	$\frac{X+1}{X_0+1}\rho_0$	kg·m^{-3}	Apparent sludge density [9]
C_p	$-2.32\exp(-1.39\left(\frac{X}{X_0}\right)) + 3.14$	J·g^{-1}·K^{-1}	Heat capacity
a_w	$1 - \exp(-0.282X^{1.823})$	-	Water activity

The apparent moisture diffusion coefficient was determined in the frame of thesis work (unpublished yet), based on reverse numerical method [5], as follows:

$$D_{app} = 10^{-8} \times \left(8888 - 8237\left(\frac{X}{X_0}\right) + 31220 \times \exp\left(-30.8\left(\frac{X}{X_0}\right)\right)\right) \times \exp\left(\frac{-26546.6}{R_{gas}T}\right)) \quad (6)$$

III. RESULTS AND DISCUSSIONS

A. Simulation of Water Content

Fig. 2 shows the simulated moisture content profiles within a 30 g sludge sample during drying. The water content is first

uniform throughout the geometry of the sample (Fig. 2 (a)). After one hour of drying, the water content is slightly reduced and is between 1.95 at the bottom and 2.04 at the top (Fig. 2 (b)). As the drying progresses, the water content decreases irregularly in the sample, creating concentric layers with increasing water contents towards the bottom of the sludge (Figs. 2 (b) and (c)). The water content continues to decrease until it reaches equilibrium X_{eq} = 0.07 after 65 hours at the end of drying (Fig. 2 (d)). These simulation results indicate that the coupling of the different equations leads the numerical model to converge appropriately to render simulation results consistent with the input data and the experimental results.

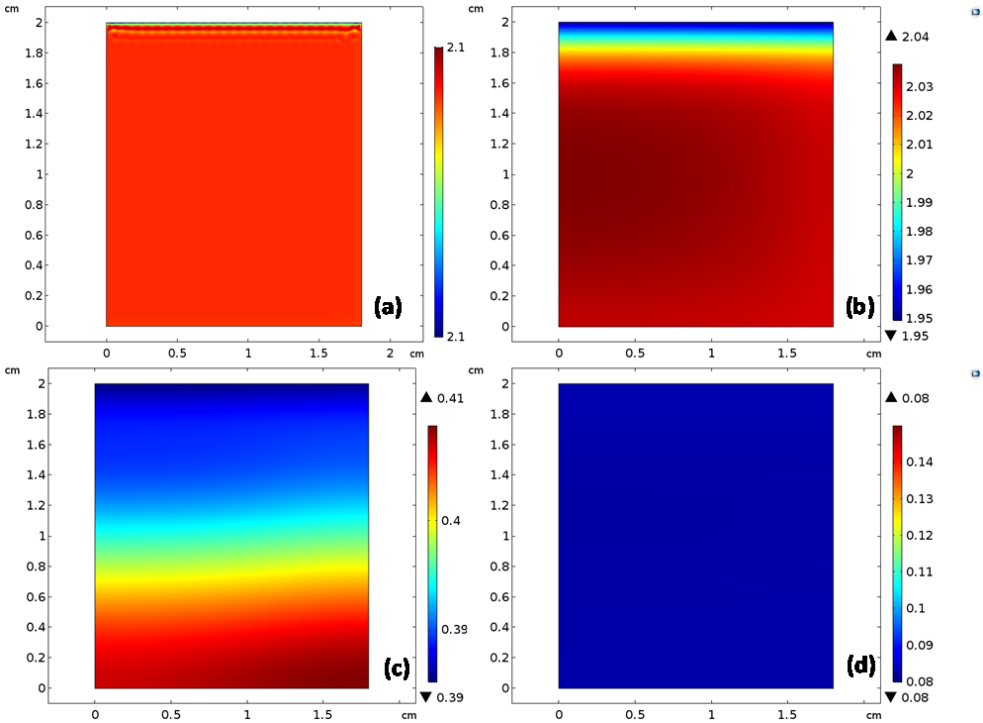

Fig. 2 Simulation results of the water content distribution in sludge sample at t = 0 h (a); t = 1 h (b); t = 35 h (c) and t = 65 h (d) (RH = 46%, 65 °C and atmospheric pressure)

B. Effects of Temperature and Pressure on Drying

A first set of 30 g samples of sludge was exposed at different temperatures (35, 45, 55 and 65 °C) to estimate the temperature effect on drying by measuring the water loss over time. A second set was exposed at different pressures (200, 350 and 1000 mbar), to determine the effect of vacuum conditions on drying. Figs. 3 (a) and (b) show respectively, the simulated and experimental drying curves acquired on samples dried at different temperatures (35, 45, 55 and 65 °C) and pressures (200, 350 and 1000 mbar). The simulated water content values X_{sim} are extracted from the 2D simulations based on the spatial average (average function in COMSOL-Multiphysics) at each time step. To estimate the concordance between the simulation results and the experimental data, R^2 and RMSE are estimated by statistical analysis. The simulated results are in good agreement with the experimental results, with an overall R^2 greater than 99.6% and RMSE lower than 0.04. On the other hand, the simulated drying curve is shifted with respect to the experimental curve, which indicates an underestimation of the drying rate in the numerical model. This is due to the fact that the phenomenon of sludge shrinkage, that was experimentally observed, is neglected until now in this model. The exchange surface in the current model is constant and equal to the top surface; therefore, the exchange surface between the sludge and the surrounding air is underestimated. Indeed, when the sludge shrinks, an additional exchange surface is created at the lateral side that promotes the evaporation. In addition, the reduction of the sludge volume boosts the transport of water in the porous medium, and therefore promotes evaporation.

These experimental results confirm the effect of high temperature on the acceleration of drying. Since the water transfer is directly proportional to the temperature (6), the drying rate in the sludge is faster at high temperature. Experiments at 1000 mbar and HR = 46% show that the required drying times to reach X/X_0= 0.05 are 43 h, 55 h, 75 h and 115 h at 65 °C, 55 °C, 45 °C and 35 °C, respectively (Fig. 3 (a)). Drying at 65 °C then gives a gain of 67% in time to reach steady state compared to drying at 35 °C. On the other hand, experimental and simulated results confirm the effect of low pressure on the acceleration of drying. Since the evaporation rate is directly proportional to the pressure gradient (3), the evaporation in the sludge is higher at low pressure and the drying rate is faster. Experiments at 65 °C and HR = 46% show that the required drying times to reach

$X/X_0 = 0.05$ are 43 h, 37 h and 27 h at 1000 mbar, 350 mbar and 200 mbar, respectively (Fig. 3 (b)). Drying at 200 mbar then gives a gain of 60% in time to reach steady state compared to drying at 1000 mbar.

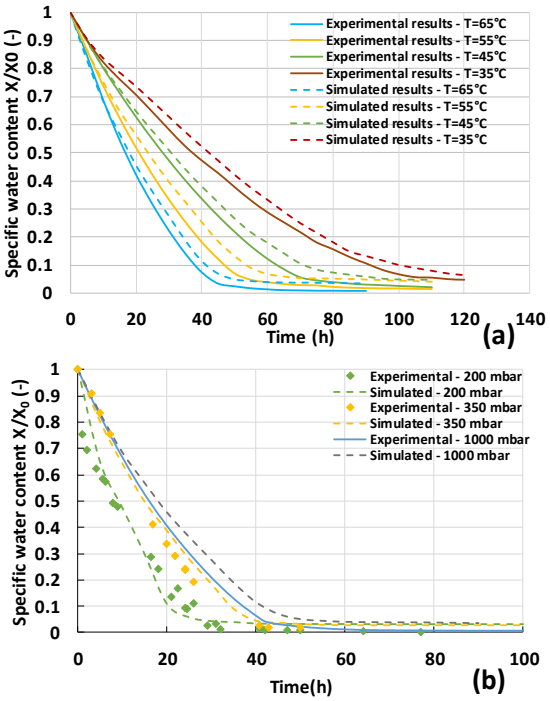

Fig. 3 Simulated water content evolution of 30 g sludge sample at RH=46%, at different (a) temperatures (under atmospheric pressure) and (b) pressures (at 65 °C)

IV. Conclusion

A numerical model has been developed to simulate the drying process and the involved mechanisms of 30 g sludge samples at different temperatures and vacuum pressures. Heat and mass transfers are taken into account. Simulated results are found concordant in the beginning, then shifted compared to the experimental results. This mismatch may be due to the shrinkage phenomena, experimentally observed but neglected in the model. Experimental and simulated results prove that drying is favored at higher temperature and lower pressure. In the next step, shrinkage will be included as a function of water content. Therefore, the final numerical model will consist of a heat and mass balance system coupled with the geometric deformation equation.

References

[1] BG Aval / DMDR - AREVA, Rapport d'avancement sur la gestion des dechets radioactifs MAVL d'AREVA, (2015).

[2] S. Louarn, J. Ploteau, P. Glouannec, H. Noel, *Experimental and numerical study of flat plate sludge drying at low temperature by convection and direct conduction*, Drying Technology. 32 (2014) 1664–1674. https://doi.org/10.1080/07373937.2014.916299.

[3] N.B. Hassine, X. Chesneau, A.H. Laatar, *Numerical modeling of heat and mass transfers under solar drying of sewage sludge*, Heat Transfer Research. 49 (2012) 327–348. https://doi.org/10.1615/HeatTransRes.2018017977.

[4] D. Wu, X. Peng, A. Su, A. Mujumdar, C. Hsu, D. Lee, *Heat and mass transfer in unsaturated porous cake with heated walls*, Drying Technology. 26 (2008) 1079–1085. https://doi.org/10.1080/07373930802179491.

[5] R. Thuwapanichayanan, S. Prachayawarakorn, S. Soponronnarit, *Modeling of diffusion with shrinkage and quality investigation of banana foam mat drying*, Drying Technology. 26 (2008) 1326–1333. https://doi.org/10.1080/07373930802330979.

[6] M. Kohout, A.P. Collier, F. Štěpánek, *Mathematical modelling of solvent drying from a static particle bed*, Chemical Engineering Science. 61 (2006) 3674–3685. https://doi.org/10.1016/j.ces.2005.12.036.

[7] M. Murru, G. Giorgio, S. Montomoli, F. Ricard, F. Stepanek, *Model-based scale-up of vacuum contact drying of pharmaceutical compounds*, Chemical Engineering Science. 66 (2011) 5045–5054. https://doi.org/10.1016/j.ces.2011.06.059.

[8] C. L. Yaws, *The Yaws Handbook of Vapor Pressure : Antoine Coefficients*, Gulf Prof. Pub., 336p, Elsevier, 2015. https://doi.org/10.1016/C2014-0-03590-3.

[9] B.K. Koua, P.M.E. Koffi, P. Gbaha, *Evolution of shrinkage, real density, porosity, heat and mass transfer coefficients during indirect solar drying of cocoa beans*, Journal of the Saudi Society of Agricultural Sciences. 18 (2019) 72–82. https://doi.org/10.1016/j.jssas.2017.01.002.